Supporting Information

Enabling the Selective Detection of Endocrine Disrupting Chemicals via Molecularly Surface-Imprinted "Coffee-Rings"

Jihye Lee,[†,§] *Jin Chul Yang*,[‡,§] *Saifullah Lone*,[†] *Woon Ik Park,*[∥] *Zhiqin Lin*,[¶] *Jinyoung Park*,[*,‡] *and Suck Won Hong*[*,†,]

[†]Department of Cogno-Mechatronics Engineering, Department of Optics and Mechatronics Engineering, College of Nanoscience and Nanotechnology, Pusan National University, Busan 46241, Republic of Korea

[‡]School of Applied Chemical Engineering, Department of Polymer Science & Engineering, Kyungpook National University, Daegu 41566, Republic of Korea

[∥] Department of Materials Science and Engineering, Pukyoung National University, Busan 48513, Republic of Korea

[¶]School of Materials Science and Engineering, Georgia Institute of Technology, Atlanta, Georgia 30332, United States

[§]These authors contributed equally to this work

*Correspondence should be addressed to J.P. (email: jinpark@knu.ac.kr) and S.W.H. (email: swhong@pusan.ac.kr)

KEYWORDS: molecularly imprinted polymer, coffee-ring, self-assembly, sensors, herbicide

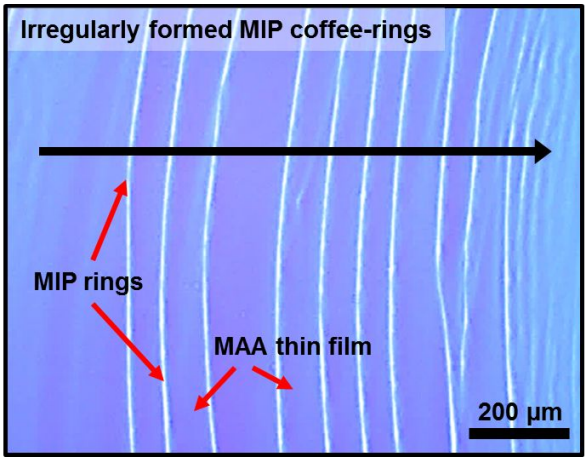

Figure S1. Optical micrograph of MIP "coffee-rings" deposited on a Si substrate without the use of a confined geometry. A conventional drop casting experiment was performed on a single surface using a MIP precursor solution (c = 0.25 mg mL^{-1}). MIP rings with irregular configuration and continuous MAA thin films were observed alternatively along with the capillary flow; the black arrow on the middle indicates the moving direction of the meniscus during the solvent evaporation.

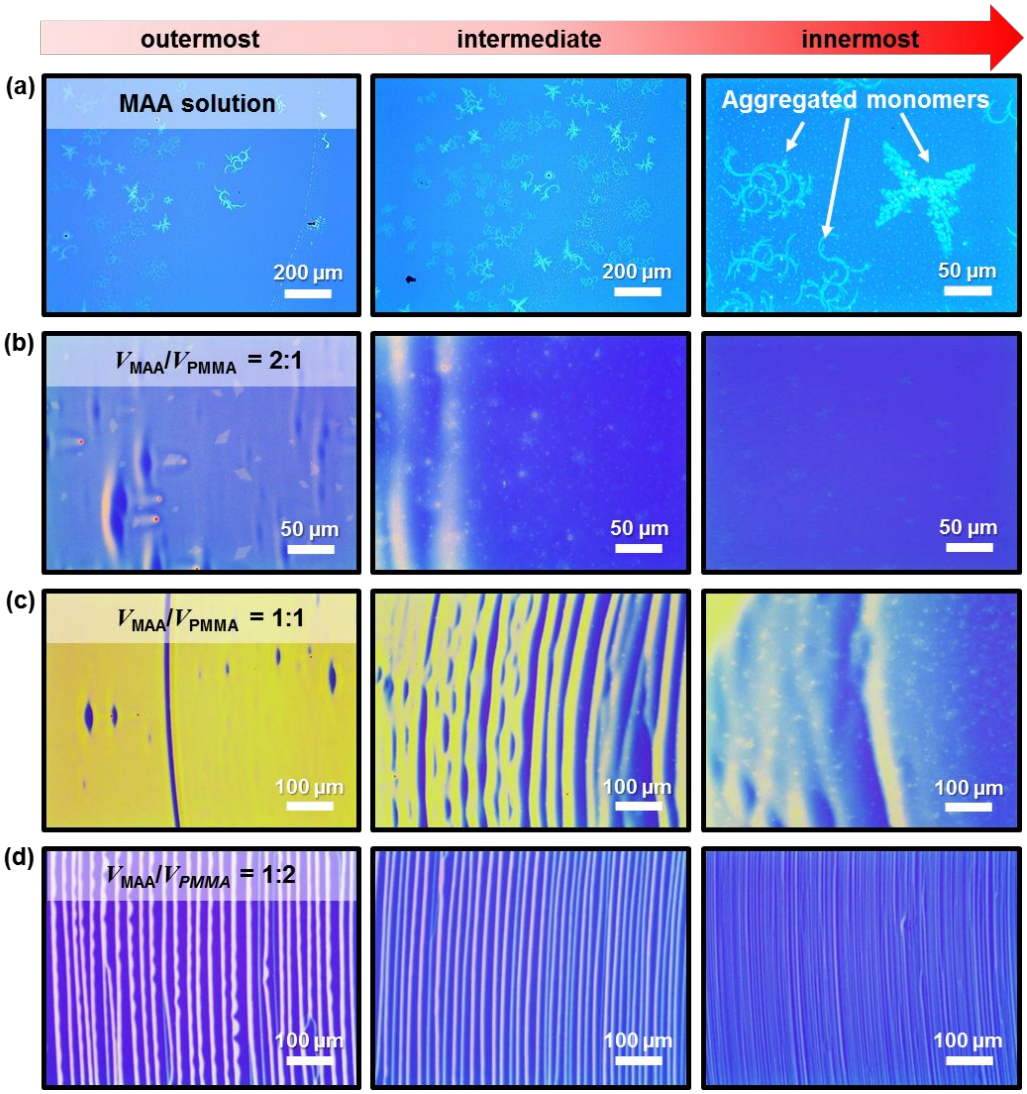

Figure S2. Optical micrographs from the results of the control experiments of the MIP precursor solution in a sphere-on-flat confined geometry; the mixing volume ratios of the MAA monomer and the linear host polymer (PMMA) were varied with the fixed solution concentration (0.25 mg mL^{-1}). (a) MMA toluene solution (without PMMA host polymer); MAA thin film was formed and some were aggregated. (b) In this case of V_{MAA}/V_{PMMA} = 2:1, the pinning of the linear base polymer was inhibited and instead, the continuous MIP thin film was formed with some perturbed wavy patterns since the influence of MAA monomer was dominant. (c)) In this case of V_{MAA}/V_{PMMA} = 1:1, some ring patterns started to appear partially in the intermediate region, but the continuous film or unwanted instabilities was mostly observed. (d)) In this case of V_{MAA}/V_{PMMA} = 1:2, the concentric MIP "coffee-rings" began to form in ordered array over the large area when the portion of linear host polymer was increased, while the edges of the MIP stripes were slightly jagged and less regular with fingering instabilities.

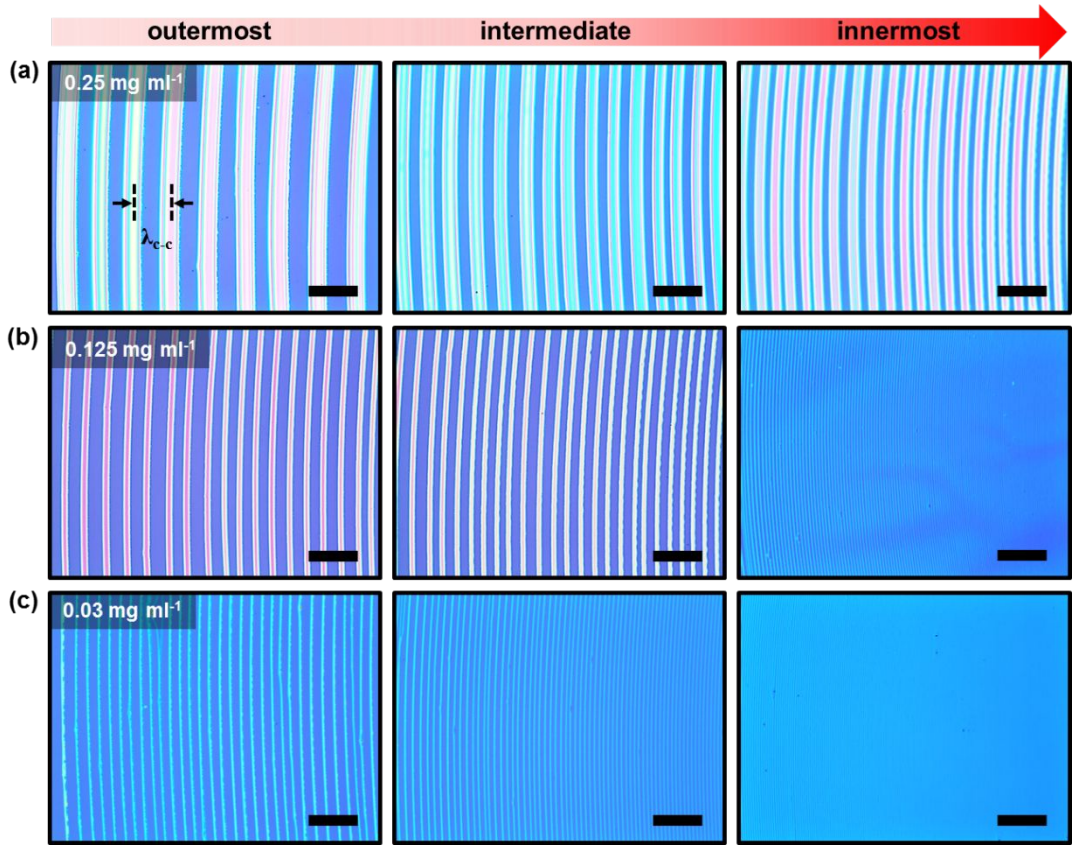

Figure S3. Optical micrographs of concentric ring patterns obtained from controlled evaporation of PMMA solution with different concentrations in sphere-on-Si geometry; each concentration of PMMA solutions was (a) 0.25 mg mL^{-1}, (b) 0.125 mg mL^{-1}, and (c) 0.03 mg mL^{-1}, respectively. The images were collected from the outermost, intermediate, and innermost region (left to right) toward the contact center. The values of $\lambda_{C\text{-}C}$ were gradually decreased as the PMMA solution moves inward into the contact center. All scale bars are 100 μm.

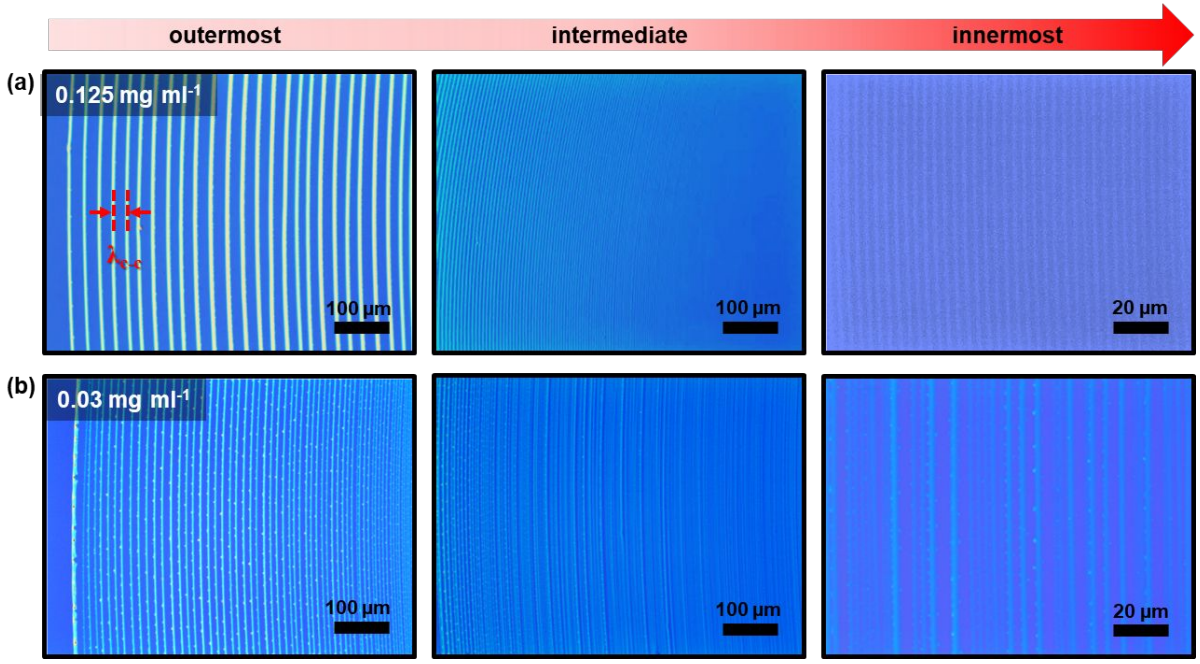

Figure S4. Optical micrographs of concentric ring patterns resulted from controlled evaporation of varied MIP precursor solutions in sphere-on-Si geometry; the concentrations were (a) 0.125 mg mL^{-1} and (b) 0.03 mg mL^{-1}. The images were collected from the outermost, intermediate, and innermost region (left to right) toward the contact center. Similar to the PMMA solution cases, the finite patterns were formed regularly, and the values of $\lambda_{C\text{-}C}$ were gradually decreased as the MIP precursor solutions moves inward into the contact center.

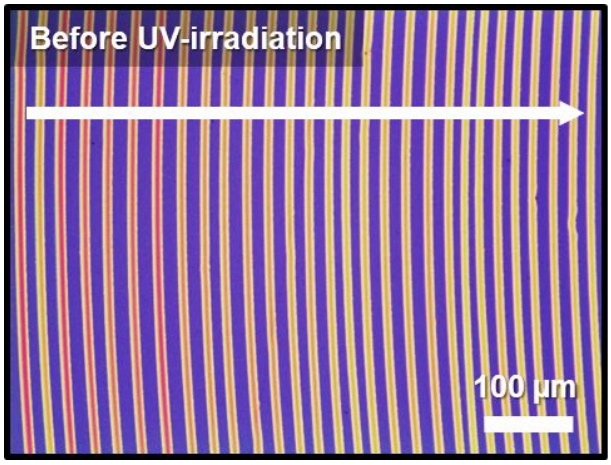

Figure S5. Optical micrograph of patterned MIP rings formed on Si substrate by evaporative self-assembly in sphere-on-Si geometry (c = 0.25 mg mL^{-1}) prior to UV-irradiation step. There were no significant morphological changes of the patterned MIP rings in the configuration before and after the UV-irradiation (Figure 2a).

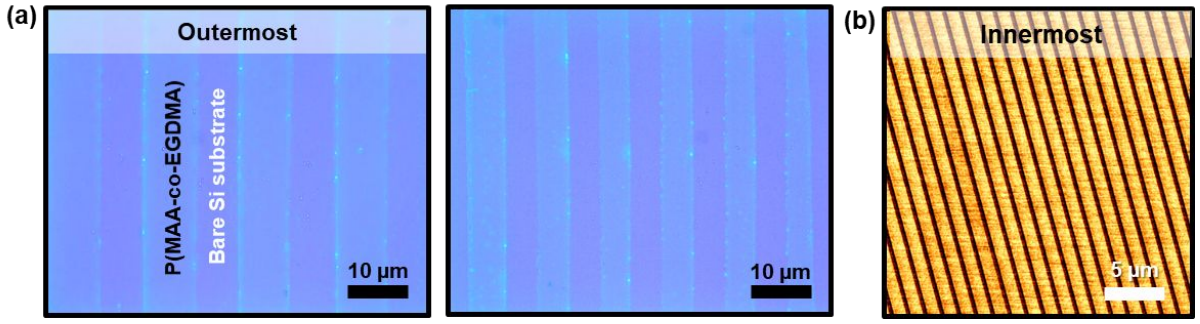

Figure S6. (a) Optical micrographs of the result from the lift-off process of the semi-IPN MIP ring patterns (schematically illustrated in Fig. 3a, right panel); the left and right images were captured form the outermost and intermediate region, respectively. (b) At the innermost region of the sample, the finite patterns of ultrathin P(MAA-co-EGDMA) stripes were measured by the AFM with extremely high regularity over a large area (i.e., the intervals of the stripes were ~400 nm); with the limited resolution in imaging, optical micrograph cannot be shown for the innermost region.

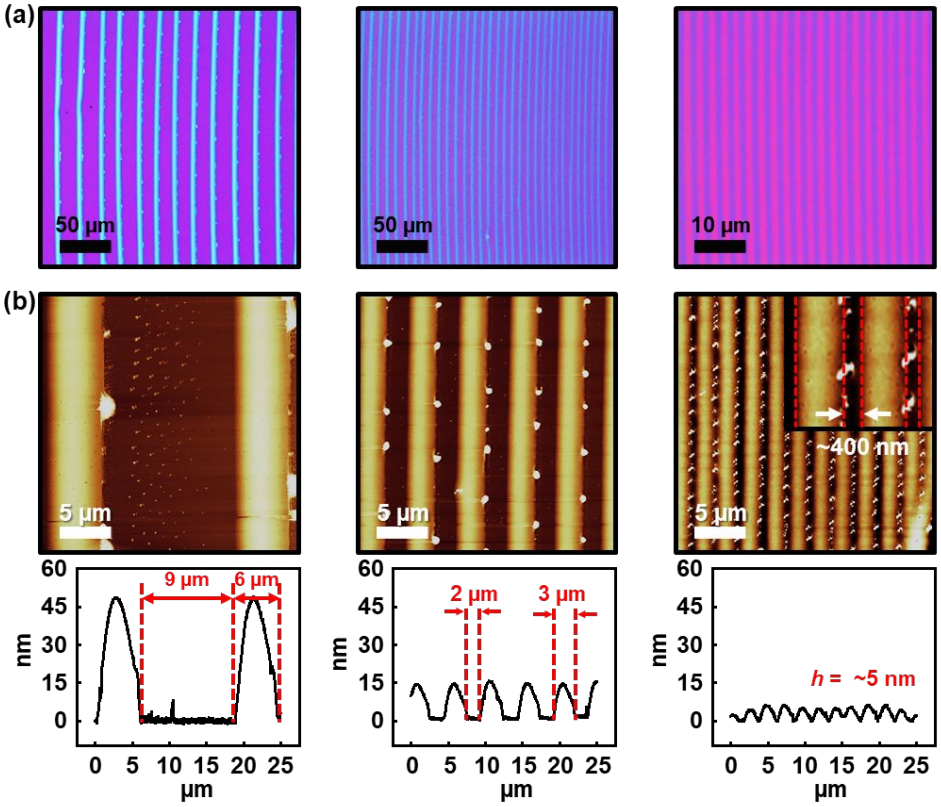

Figure S7. (a) Optical micrographs of ring-patterned MIP film formed by evaporative self-assembly (c = 0.5 mg mL^{-1}). The images were collected from the outermost to innermost region toward the contact center. (b) AFM images and corresponding height profiles from the center locations in (a); the heights of the MIP rings were measured to be ~48 nm, ~15 nm, and ~5 nm, respectively.

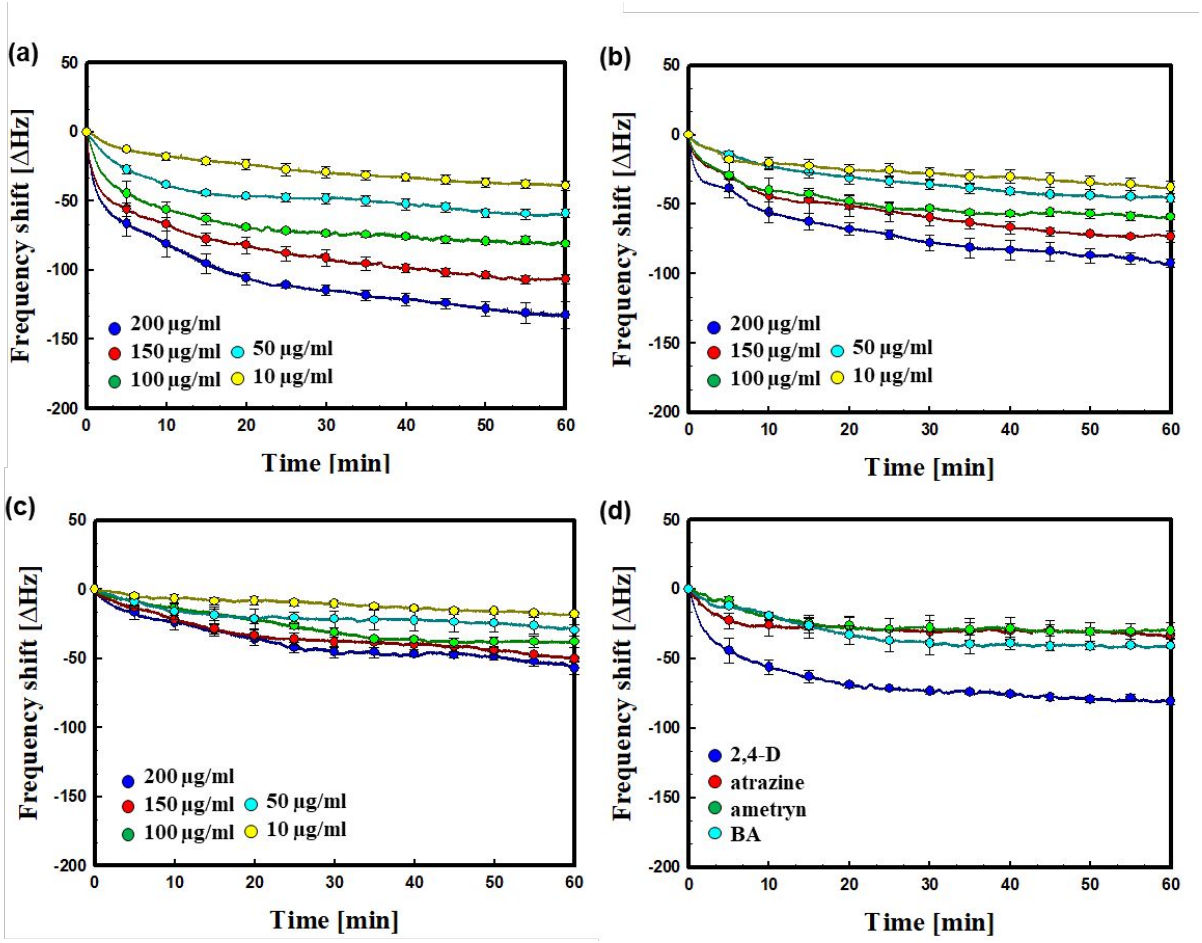

Figure S8. Resonant frequency changes as function of elapsed time for (a) ring-patterned MIP, (b) planar MIP, and (c) ring-patterned NIP films during the rebinding process in range of concentration from 10 to 200 µg mL^{-1} of 2,4-D. (d) Resonant frequency change as function of elapsed time using the ring-patterned MIP films for the detection of herbicides; the tests for the selectivity were performed in the fixed concentration (i.e., 100 µg mL^{-1}) of each herbicides (2,4-D, atrazine, ametryn, and BA) for 60 min.